POLITECNICO DI TORINO
Repository ISTITUZIONALE

Hyperspectral Characterization of Coffee Leaf Miner (Leucoptera coffeella) (Lepidoptera: Lyonetiidae) Infestation Levels: A Detailed Analysis

Terms of use:

(Article begins on next page)

22 February 2025

Article

Hyperspectral Characterization of Coffee Leaf Miner (*Leucoptera coffeella*) (Lepidoptera: Lyonetiidae) Infestation Levels: A Detailed Analysis

Vinicius Silva Werneck Orlando [1,*], Maria de Lourdes Bueno Trindade Galo [1], George Deroco Martins [2], Andrea Maria Lingua [3], Gleice Aparecida de Assis [4] and Elena Belcore [3]

[1] Postgraduate Program in Cartographic Sciences, São Paulo State University, Presidente Prudente 19060-900, SP, Brazil; trindade.galo@unesp.br

[2] Institute of Geography, Federal University of Uberlândia, Monte Carmelo 38500-000, MG, Brazil; deroco@ufu.br

[3] Department of Environment, Land and Infrastructure Engineering (DIATI), Politecnico di Torino, 10129 Torino, Italy; andrea.lingua@polito.it (A.M.L.); elena.belcore@polito.it (E.B.)

[4] Institute of Agricultural Sciences, Federal University of Uberlândia, Monte Carmelo 38500-000, MG, Brazil; gleice@ufu.br

[*] Correspondence: vinicius.werneck@unesp.br

Abstract: Brazil is the largest coffee producer in the world. However, it has been a challenge to manage the main pest affecting the plant's foliar part, the Coffee Leaf Miner (CLM) *Leucoptera coffeella* (Lepidoptera: Lyonetiidae). To mitigate this, remote sensing has been employed to spectrally characterize various stresses on coffee trees. This study establishes the groundwork for efficient pest detection by investigating the spectral characteristics of CLM infestation at different levels. This research aims to characterize the spectral signature of leaves at different CLM levels of infestation and identify the optimal spectral regions for discriminating these levels. To achieve this, hyperspectral reflectance measurements were made of healthy and infested leaves, and the classes of infested leaves were grouped into minimally, moderately, and severely infested. As the infestation level rises, the 700 nm region becomes increasingly suitable for distinguishing between infestation levels, with the visible region also proving significant, particularly during severe infestations. Reflectance thresholds established in this study provide a foundation for agronomic references related to CLM. These findings lay the essential groundwork for enhancing monitoring and early detection systems and underscore the value of terrestrial hyperspectral data for developing sustainable pest management strategies in coffee crops.

Keywords: spectral signature; precision agriculture; pest management

1. Introduction

Coffee is one of the most consumed beverages globally and one of the most traded commodities worldwide, and Brazil is the largest coffee producer in the world. Nevertheless, climate change has significantly affected tropical regions and their crops, including coffee. As a result, coffee has been included in Climate Smart Agriculture (CSA) strategies. This decision follows projections that indicate an increase in the prevalence of pests that increase in drought conditions [1]. Indeed, the alteration of climatic conditions in various parts of the world leads to ecosystem imbalances, often resulting in the proliferation of previously less impactful or absent pathogens. This is the case with the Coffee Leaf Miner (CLM), *Leucoptera coffeella* (Lepidoptera: Lyonetiidae) [2,3], a monophagous pest that exclusively affects coffee plants, which is the main foliar pest that develops during the dry period in Brazil.

In the caterpillar stage of the CLM, it causes necrotic lesions on the leaves, followed by the shedding of mined leaves from the top of the plants. The presence of mines triggers

multiple physiological responses: it increases ethylene production (a plant hormone responsible for leaf abscission) [4], reduces photosynthetic area and auxin levels [5,6], and leads to chlorosis that can take over the entire leaf. These effects can result in yield losses of 30% to 70% [2] or even plant death.

Currently, CLM monitoring in coffee plantations is conducted through systematic field sampling, where the average number of mines per plant is counted using a zigzag pathway or regular sampling grid [7,8].

To facilitate field detection, systems that utilize remote sensing technology are currently being developed [2]. Several authors indicate that remote sensing has been a more sustainable and accurate methodology in the discrimination of stresses in agriculture [9–11], especially in coffee crops [12–16]. Considering the operational challenges associated with cultivating coffee crops on extensive terrains, particularly in the Cerrado region of Minas Gerais, employing remote sensing emerges as a swifter strategy for CLM detection. However, despite their growing prevalence, remote sensing techniques are underutilized in this area.

To effectively monitor the phytosanitary status of a plantation or an entire region using remote sensing, it is essential to accurately characterize how the crop's spectral response varies with the intensity of stress from biotic or abiotic disturbances. When dealing with spectroscopy and hyperspectral measurements, the main challenge is to develop a methodology that correlates the agronomic assessment of infested crops with hyperspectral measurements and discriminates the best intervals for classifying disease intensity.

Therefore, characterizing the spectral signature of CLM-infested leaves at different stages of infestation becomes crucial for timely intervention before the plant suffers severe defoliation. By accurately delineating the spectral patterns of CLM-infested leaves, coffee producers can create precise predictive tools capable of anticipating the widespread attack of their production area.

Researchers have taken up this challenge in recent years, mainly due to the devastating nature of the effects of CLM. However, most studies utilizing remote sensing techniques have relied on medium-resolution satellite images (e.g., Sentinel-2 constellation, with a spatial resolution of approximately 10–20 m) with a solid CLM spectral response knowledge. Ref. [15] developed the "Coffee-Leaf-Miner Index" (CLMI), which combines the near-infrared, blue, and red bands for detecting CLM infestation at orbital images from Sentinel-2. A determination coefficient of 0.87 and an accuracy of 89.47% were achieved, highlighting the importance of red and near-infrared (NIR) ranges. More recently, Ref. [17] demonstrated that the random forest algorithm effectively identified healthy or infested areas by CLM, using indices derived from Sentinel-2 images. The results achieved an accuracy of 86% and a kappa index of 0.64.

To the authors' knowledge, there is limited research on higher resolution and, currently, there is no literature describing a strategy to quantify damage levels on individual leaves that could serve as an indicator for estimating the impact of CLM on the entire field. This information could significantly enhance detection using higher-resolution optical imagery, such as those collected by Unmanned Aerial Vehicles (UAVs) or very high-resolution optical satellite constellations, facilitating a more efficient detection of CLM.

In this context, this research aims to define the hyperspectral response of leaf miners. It not only addresses a critical gap in the current scientific literature, it also has profound implications for advancing agricultural practices in the coffee industry.

It is hypothesized that hyperspectral remote sensing can discriminate the different infestation levels of CLM in the leaves using specific regions of the electromagnetic spectrum. This study aims to comprehensively characterize the hyperspectral signature of leaves across varying CLM-infestation levels, aiming to (i) identify and delineate the optimal spectral regions that effectively discriminate between different degrees of infestation; (ii) to define an agronomic reference for CLM degree on infestation at leaf-level; and (iii) cluster CLM-infestation intensity according to the reflectance.

2. Materials and Methods

The study was carried out in an experimental coffee area located on the Monte Carmelo Campus of the Federal University of Uberlândia, and consists of one plot with 3.5 m spacing between rows, 0.6 m between plants, and an average height of 2 m (Figure 1). The area has approximately 200 coffee trees in 650 m^2 and is drip irrigated. The site has an average annual rainfall of 1444 mm and a climate classified as tropical with a dry winter, which is the main condition for the natural development of the investigated pest. The experimental area was composed of *Coffea arabica* L. with cultivar Topázio MG-1190, which is susceptible to CLM attack.
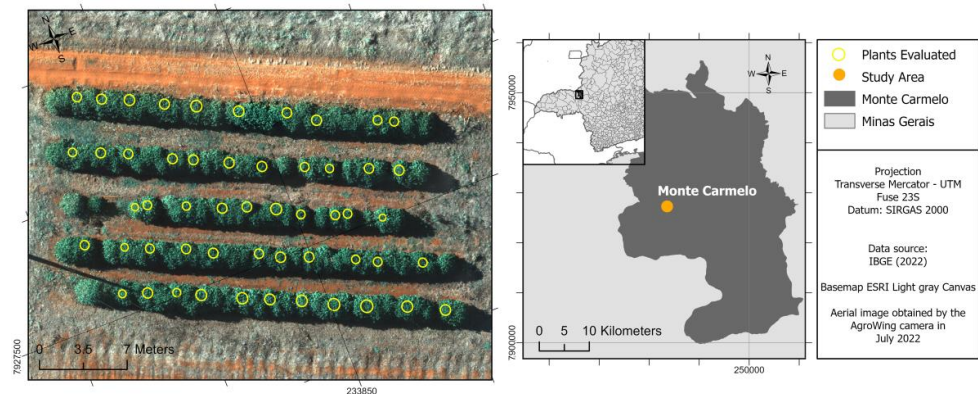
Figure 1. Location of the experimental area and an aerial image of the investigated coffee tree plot.

To evaluate the hypothesis that remote sensing can be used to discriminate different clusters of leaf miner attacks, the flowchart in Figure 2 was proposed. Radiance measurements were obtained from 80 healthy and 80 infested leaves, specifically those affected by stress caused by the leaf miner pest. These values were subsequently transformed into the Hemispherical Conical Reflectance Factor (HCRF).
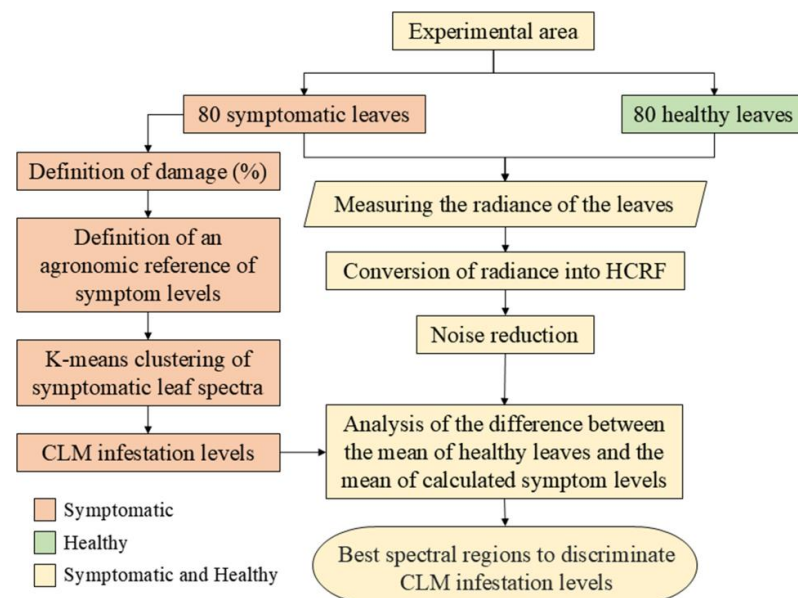
Figure 2. Overall flowchart of the methodology.

However, for an assessment at the leaf-level, it was necessary to create a new agronomic reference which included the percentage of damage on the mined leaf. Subsequently, the k-means clustering algorithm was employed to explore the optimal number of categories for discriminating among the 80 leaves, using the percentage of symptoms as a

reference. Then, analysis of variance (ANOVA) was used to determine whether the mean HCRF of infested leaves had a significant difference when compared to the mean HCRF of healthy leaves. In this sense, three graphs were generated to explore the most important spectral regions for detecting the miner at different infestation levels.

2.1. Data Acquisition

2.1.1. Identification and Field Collection of Healthy and Symptomatic Leaves

The evaluation of injuries by leaf miners was carried out in July 2022, a period of lower relative humidity with an average relative humidity of 58% [18], and considered suitable for the emergence of CLM. For this, 160 leaves located on the third or fourth pair of randomly chosen plagiotropic branches in the middle/upper third of the plant were removed, following the same methodology that is applied for evaluation in whole plants, and these were classified as healthy (80 leaves) and symptomatic (80 leaves).

2.1.2. Acquisition of Hyperspectral Measurements of the Leaves

Leaves, removed from the plants, were fixed above a black non-reflective target to minimize the influence of radiation from neighboring surfaces on the spectral radiance measurements of the leaves. The measuring instrument was a FieldSpec® Handheld spectroradiometer from Analytical Spectral Devices (ASD, Boulder, US), which operates in the spectral range of 325–1075 nm, with a spectral resolution of 1.6 nm. A filter limiting the field of view (FOV) to 10° was coupled with a distance from the spectrum to the leaf of approximately 114 mm, obtaining an instantaneous field of view (IFOV) of 10 mm.

For every leaf radiance measurement, an average of ten repetitions of the target radiance reading and the radiance of a reference Lambertian surface (Spectralon plate) [19] were concurrently measured under the same lighting and observation conditions, between 11 a.m. and 2 p.m. (Figure 3A).
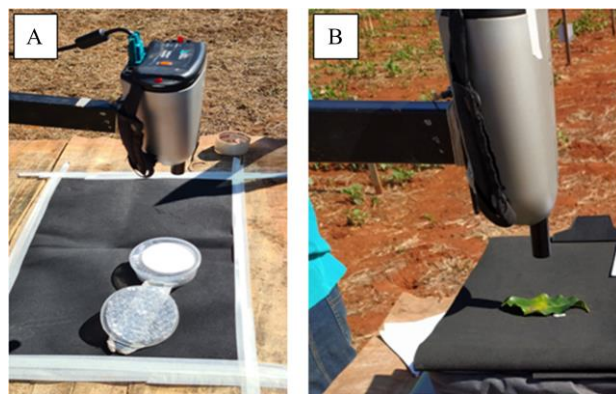
Figure 3. Hyperspectral measurements in the field. (**A**) Spectralon plate, (**B**) symptomatic coffee leaf.

The sensor was pointed at the adaxial surface of the leaf (upper part), measuring the spectral signature of the central part of the leaf (Figure 3B), with 80 symptomatic and 80 healthy leaves.

2.2. Data Processing

2.2.1. Determining the Percentage Level of Leaf Damage

The level of leaf damage due to leaf miner attack was calculated as a function of the percentages of injury and yellowing of the leaves. For that, the symptomatic leaves were photographed using a conventional cell phone camera. The images were processed in AFSoft 1.1, a specific software for leaf analysis developed in Brazil [20] based on a supervised neural network that calculates the percentages of (1) mined, (2) green/healthy, and (3) yellow/chlorotic areas. The percentages were calculated based on the total leaf area, without taking the dimensions in centimeters into account.

2.2.2. Clustering of Infestation Levels by K-Means

The clustering process was based on the percentages of leaf damage caused by CLM and the yellowing areas. These percentages, representing the extent of damage, were used to determine the optimal number of clusters. The k-means clustering algorithm was implemented in Python using the scikit-learn library to categorize infestation levels into distinct clusters. The ideal number of clusters was determined using the elbow method and the Silhouette Index. The elbow method entails examining the angles formed by the root mean squared error (RMSE) values across various numbers of clusters (k) tested. The optimal k is identified at the point where further additions of clusters do not yield a significant reduction in RMSE. However, a comparative analysis with another method becomes essential to bolster this decision-making process in determining the number of centroids. In this context, the Silhouette Index method [21] was employed to ascertain the optimal number of clusters. This method is particularly valuable as it assesses the quality of clusters by considering individual points situated among multiple clusters.

As the k-means algorithm is sensitive to the scale of the data, a normalization technique was employed on the original data values (X). The StandardScaler (Equation (1)) from the scikit-learn library was used to perform this normalization. This method transforms the data such that each feature has a mean (μ) of 0 and a standard deviation (σ) of 1, and does not restrict values within the range -1 to 1. Transformed values may extend beyond this range, but all variance in the data is preserved, allowing the clustering algorithm to capture the inherent structure of the data more effectively.

$$X_{normalized} = \frac{X - \mu}{\sigma} \tag{1}$$

2.2.3. Hyperspectral Processing of Measurements

The HCRF, given by Equation (2), is determined by the ratio between the average radiance (L target) reflected by the target and that of an ideal diffusing surface (L surface), represented by a Spectralon plate, under identical geometric and lighting conditions, as demonstrated in [13]. As the Spectralon plate used in the field deviates from the ideal conditions of a laboratory diffusing surface, a calibration factor (k) was calculated in reference to a perfectly conditioned plate available in the laboratory.

$$HCRF = \left(\frac{L_{target}}{L_{surface}}\right) \times k \tag{2}$$

Aiming to reduce noisy values, the spectral range of 400 to 1000 nm was used, and a 7 nm (points) mean filter was applied to the data to smooth the spectral signatures. A mean filter takes the average spectral value of all points within the specified window as the new center point value [22].

2.2.4. Analysis and Validation Between Groups of Symptomatic and Healthy Leaves

An ANOVA test for 95% confidence level was used to analyze the significance difference between the mean spectrum levels of symptomatic leaves of each cluster and the mean of healthy leaves. The *p*-value and f-value were computed. After significance analysis, the absolute difference ($\Delta_{spectra}$) between the average HCRF of healthy leaves (HCRF_healthy) and the HCRF of each group (K) of symptomatic leaves (HCRF_symptomatic) was performed, Equation (3), to compare the best spectral regions to discern each symptom level. Then, the identification of ideal spectral regions to discern symptom levels is assessed by graphing the differences between the mean spectral behavior of healthy leaves and the mean spectral behavior of the clusters.

$$\Delta_{spectra}(K) = \left| HCRF_{healthy} - HCRF_{symptomatic} \right| \tag{3}$$

3. Results

3.1. CLM Infestation Level Based on Percentage of Leaf Damage

Figure 4 shows the results obtained using AFSoft to classify coffee leaves under different infestation conditions.
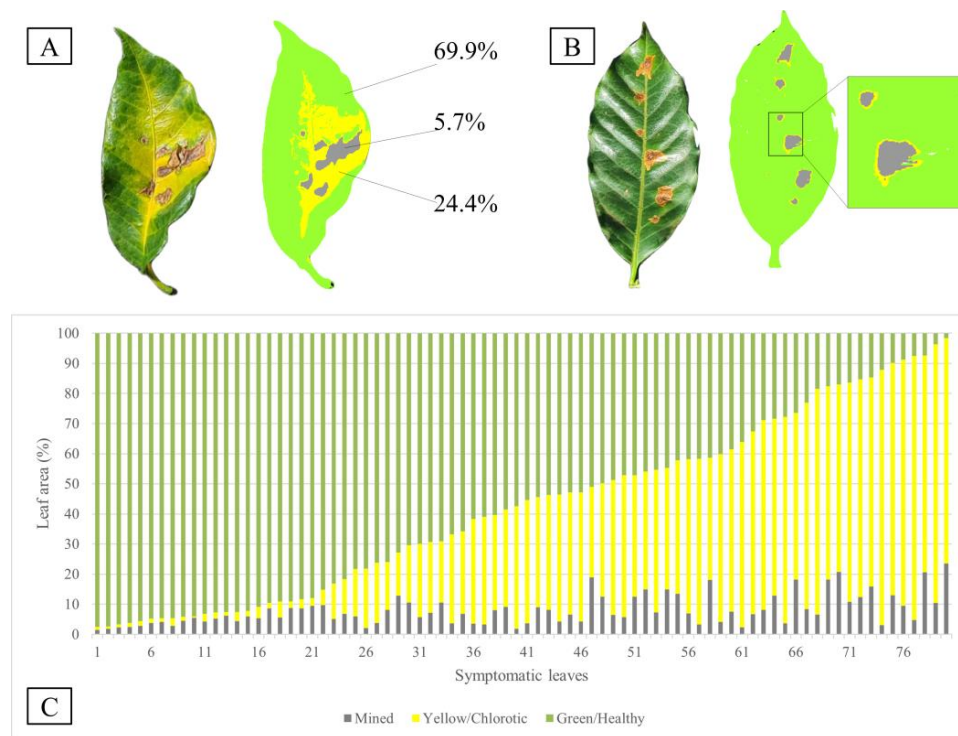

Figure 4. Classification results of coffee leaves infested by CLM using AFSoft. (**A**) Visual representation and corresponding percentage distribution of mined, yellow/chlorotic, and green/healthy areas in a symptomatic leaf. (**B**) Demonstrates the ability to detect yellowing regions adjacent to mined areas, even in leaves with lower infestation levels. (**C**) Bar chart summarizing the percentage distribution of mined, yellow/chlorotic, and green/healthy areas across all evaluated symptomatic leaves.

The classification was able to determine distinct regions of mining and chlorosis (Figure 4A) and was effective in detecting regions of subtle yellowing adjacent to mined areas, even in cases of lower severity (Figure 4B). Although the AFSoft software does not directly provide accuracy metrics for the classification model, a rigorous review of the classification outputs for each leaf was conducted to validate the results. Furthermore, the comprehensive analysis of all evaluated leaves (Figure 4C) reveals consistent detection of mined, yellow/chlorotic, and green/healthy areas, demonstrating the robustness of the classification process across varying infestation levels.

Figure 5 illustrates selecting the ideal number of clusters, using the elbow method (Figure 5A) and the Silhouette Index (Figure 5B).

In Figure 5A, the elbow method demonstrates that, after three clusters, the reduction in RMSE becomes minimal, suggesting an optimal K value around three. Moreover, this point presents the highest possible Silhouette Index (Figure 5B), underscoring that the clusters within the dataset are well-defined and distinct from one another. In this sense, the dataset was segmented into three clusters, selecting K = 3.

Table 1 highlights the main results of k-means clustering: Cluster 1, comprising 33 leaves with minimal infestation; Cluster 2, consisting of 28 leaves with moderate infestation; and Cluster 3, encompassing 19 leaves with severe infestation.
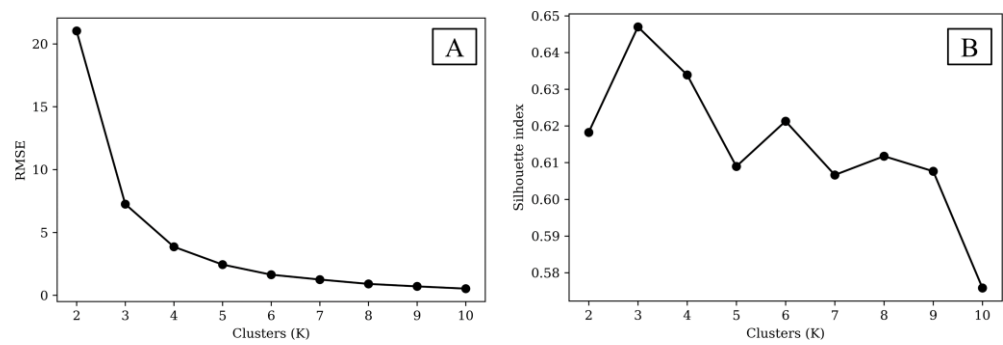
Figure 5. Selection of the best k values (**A**) The elbow method indicating that beyond three clusters, there is no significant reduction in RMSE and (**B**) Silhouette Index determining the highest value for three clusters.

Table 1. K-means clustering results in three clusters. Cluster 1 is minimally infested, Cluster 2 is moderately infested, and Cluster 3 is severely infested.

Cluster	Number of Observations	Average Distance from Centroid	Maximum Distance from Centroid
1	33	0.2742	0.6086
2	28	0.2392	0.5580
3	19	0.2528	0.5479

For Cluster 1, the average distance of observations to the centroid was 0.2742, with a maximum distance of 0.6086, with most observations relatively close to the centroid, though some variability is present. In Cluster 2, the average distance to the centroid was lower at 0.2392, with a maximum distance of 0.5580, indicating a more compact cluster. However, the range of leaf symptom percentages was broad, pointing to some heterogeneity within the cluster. For Cluster 3, the average distance was 0.2528, with a maximum distance of 0.5479. Then, Figure 6 shows the plotting of the percentage of damage to respect the defined clusters.
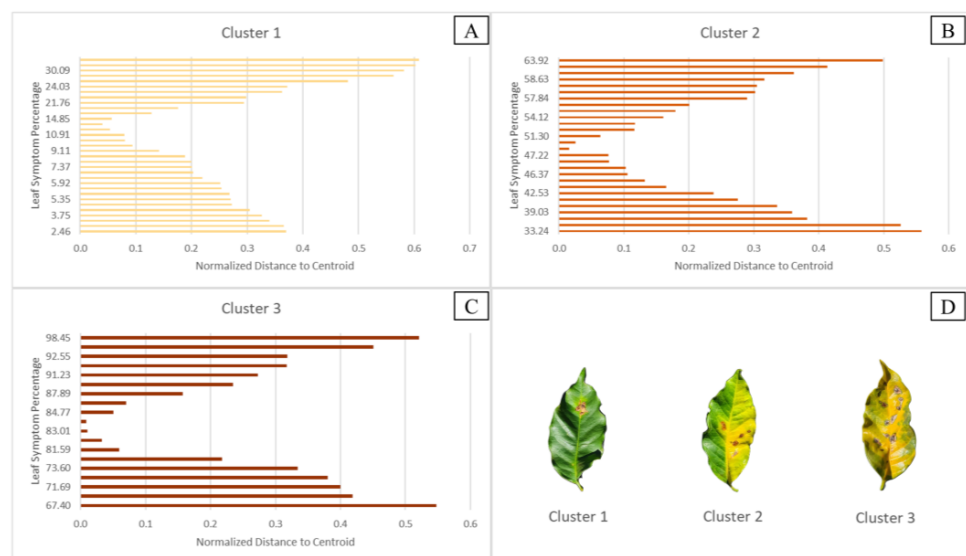

Figure 6. Symptomatic Leaves: Distribution and Distance from Cluster Centroids. (**A**) Cluster 1 is minimally infested and contains 33 leaves, (**B**) Cluster 2 is moderately infested and contains 28 leaves, (**C**) Cluster 3 is severely infested and contains 19 leaves, and (**D**) examples of leaves from each evaluated cluster, illustrating the different levels of infestation.

The normalized distances in the bar chart show the noticeable variability in leaf symptom percentages, suggesting diverse conditions or influences within this cluster. The smaller number of observations in Cluster 3 may indicate that it captures a more specific or more extreme subpopulation within the set of symptomatic leaves.

3.2. Spectral Characterization of Healthy and Symptomatic Leaves

The HCRF of healthy and symptomatic leaves were plotted, as shown in Figure 7A, while in healthy leaves, the standard spectral behavior of healthy vegetation is observed. As expected, symptomatic leaves do not show the same behavior. The overall configuration of the visible spectra indicates higher mean HCRF values in symptomatic leaves compared to healthy leaves, as shown in Figure 7B.
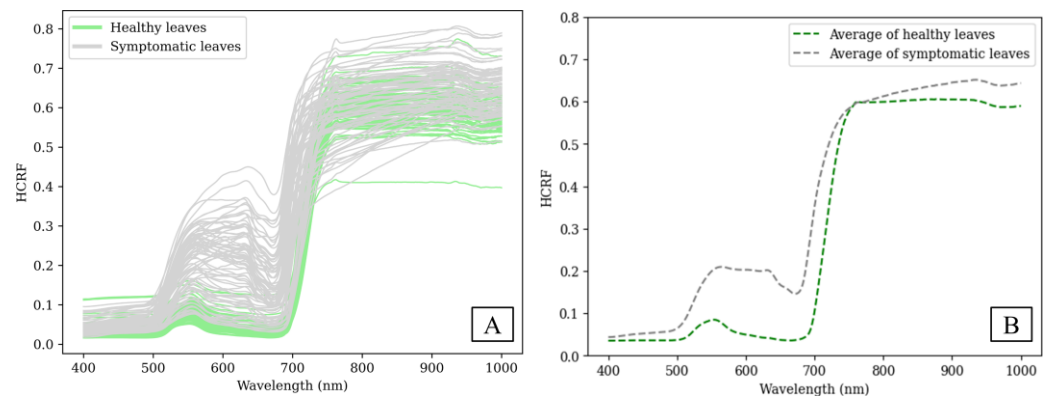
Figure 7. Healthy leaves in green and symptomatic leaves in gray. (**A**) All spectra of healthy and symptomatic leaves and (**B**) average of healthy and symptomatic leaves.

As expected, healthy coffee leaves have low reflectance in the blue (470 nm) and red (680 nm) range of the spectrum due to chlorophyll absorption, with a higher rate of reflectance in the green (560 nm). Symptomatic leaves present similar characteristics to stressed plants, with similar HCRF between the green and red regions, resulting from the decrease in leaf chlorophyll content. A distinction between the three levels of infestation is evident in the different spectral signatures of symptomatic and healthy leaves, as illustrated in Figure 8.
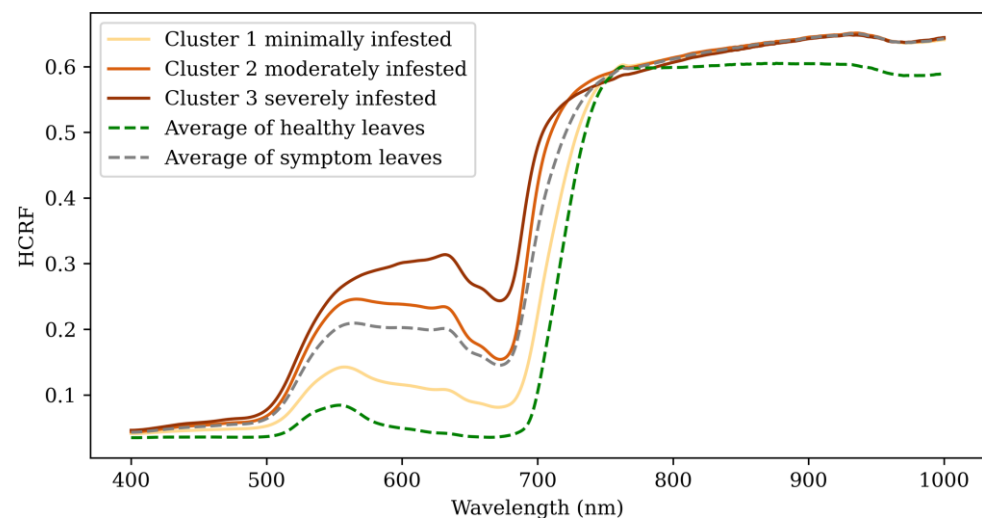
Figure 8. The average spectra of the three symptom levels are presented in solid lines. The mean spectra of healthy leaves and symptomatic leaves are shown in dotted lines.

The spectral signature of the minimally infested leaves is similar to the signature of healthy leaves, having higher HCRF in the visible spectrum region and a similar slope around 700 nm, as occurs when comparing the moderately infested leaves and the average spectrum of the infested leaves. Severely infested leaves have the highest HCRF in the visible region. This cluster also has a substantial and early increase in HCRF in the region before 700 nm.

3.3. Comparison of Average HCRF Between Symptomatic and Healthy Leaves

The symptomatic and healthy leaves groups were compared through the ANOVA test, using the average of healthy leaves as a reference. Table 2 presents the ANOVA test results for clusters 1, 2, and 3 when compared to the healthy leaf dataset.

Table 2. ANOVA test using the average of healthy leaves as a reference average healthy cluster.

Cluster	Average Healthy	
	F-Test	*p*-Value
1	6.4657	1.11×10^{-2}
2	30.3613	4.38×10^{-8}
3	48.1845	6.33×10^{-12}

Table 2 demonstrates that it is possible to differentiate between leaves infested at various levels based on the average number of healthy leaves, as indicated by the significant *p*-values. All comparisons between infestation levels and the average number of healthy leaves are statistically significant. Furthermore, the F-Statistic increases with the severity of the infestation, suggesting that the differences between clusters and the average number of healthy leaves become more pronounced with greater symptom severity.

In this sense, the result of $\Delta_{spectra}$ (K), which compares the differences between the mean of healthy leaves and the symptomatic levels, can be seen in Figure 9.
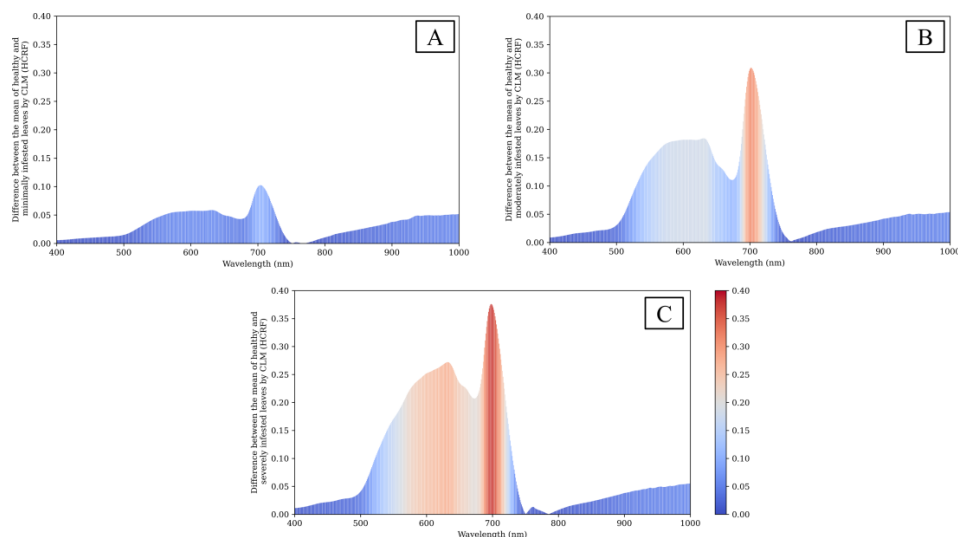
Figure 9. Analysis using the absolute differences between the mean of healthy leaves and the mean of (**A**) minimally, (**B**) moderately, and (**C**) severely infested leaves.

The largest differences have been recorded in 700 nm. Indeed, this emerges from the observation of Figure 9A, where it is possible to see that the 700 nm region, the red edge, presents the greatest difference between the minimally infested and healthy leaves. This spectrum region becomes more relevant for discriminating between healthy and infested leaves as the leaves become more infested and the differences increase significantly, as can be seen in Figure 9B,C. Furthermore, as the level of infestation increases, the visible

region, especially around the 600 nm wavelength, proves to be relevant for discriminating infestation levels.

4. Discussion

The study of the hyperspectral response of leaves affected by varying intensities of CLM, a defoliator of coffee plants causing significant production and economic losses in Brazil, revealed that the region around 700 nm in the electromagnetic spectrum is the most indicative of CLM infestations. These findings also underscore the robustness of studies conducted using satellite remote sensing. For instance, the previously mentioned study by [17] utilized data from the Sentinel-2 satellite, which is equipped with the Multispectral Instrument (MSI), and achieved promising results with random forest models which identified the 700 nm wavelength as the most critical in the model. Similarly, using a UAV and a multispectral sensor, ref. [23] found that spectral variance for CLM detection at the canopy level began to be significant from the 710 nm band.

As shown in Figure 9, the most significant spectral differences are observed at approximately 700 nm. The work by [15], which used Sentinel-2 images and the MSI sensor to develop the CLMI index, employs the NIR, red, and blue bands, achieving remarkable results. The blue band in the differences between the mean of healthy leaves and the symptomatic levels $\Delta_{spectra}$ (K) analyses was not significant, but this wavelength is strongly influenced by the atmosphere, which might explain its importance for a satellite-based indicator but not for our study. While satellite imagery typically has pixel dimensions in the order of meters, the leaf measurements were conducted using narrow spectral regions. This difference in spatial resolution between satellite sensors and high-resolution measurements could influence the comparative results.

A more detailed analysis of the $\Delta_{spectra}$ (K) shows that the red edge region is the most effective spectral band for distinguishing CLM infestations. Its importance increases as the level of infestation on the leaves rises. There is a significant increase in the reflectance of the spectrum of healthy leaves around 700 nm. As described by [24], this point marks the transition between the process of absorption by chlorophyll in the red region and the process of scattering in the near-infrared, which is influenced by the internal structure of the leaves.

In the near-infrared range, the smallest difference between the spectra is observed around 750 nm, as is clearly visible in Figures 8 and 9, where an overlap occurs that makes it impossible to differentiate between healthy and symptomatic leaves. In a previous study by [25], which focused on the detection of nematodes in coffee plants, there was also a portion of the near-infrared region where the spectra of healthy and symptomatic coffee leaves coincided. However, after overlapping and contrary to what was observed in Figure 7B, the mean HCRF of healthy leaves was higher than that of symptomatic leaves. In our results, this region proved to be incapable of discriminating the levels of infestation on the leaves. These findings suggest that the NIR spectral region, often employed for computing vegetation health indices such as Normalized Difference Vegetation Index (NDVI), is not significant in CLM.

It is possible to observe an increase in the importance of the visible region for discriminating infested leaves as they become more infested. It was observed by [26] that powdery mildew, a fungal disease that affects beet leaves, showed an increase in reflectance throughout the visible and near-infrared spectrum. Furthermore, it was found that the higher the infection level, the higher the reflectance and the greater the distance between the average spectra.

These findings are groundbreaking in the literature on remote sensing and CLM concerning infestation levels. The three identified clusters demonstrate significant differences from the sample of healthy leaves, as shown in Table 2. Here, the *p*-values are substantially below the significance thresholds, and the F-scores are consistently high across all clusters. The group of minimally infested leaves reflects greater variation in infestation levels or other monitored characteristics (Figure 6A). The group of moderately infested leaves has

the smallest average distance between the three clusters, possibly indicating a more similar level of infestation among the leaves in this group (Figure 6B). Additionally, the smaller number of observations for severely infested leaves (Figure 6C) was expected due to the characteristic defoliation of coffee plants caused by the pest attack [2,4]. This supports the selection of K = 3 for clustering the HCRF dataset of symptomatic leaves and is reinforced by the positive results of the Silhouette Index and the Elbow Method (Figure 5).

A significant challenge in this study was the absence of established agronomic references that define CLM infestation levels and their association with spectral response variations. This limitation led us to conduct the study in a single controlled experimental area of limited dimensions, where CLM occurrence was confirmed and other plant stresses were controlled. Future research will focus on expanding the dataset and exploring additional case studies to generalize the application, leveraging this initial foundation towards establishing comprehensive agronomical references.

While orbital data are utilized for extensive and continuous monitoring of plantations, leaf-level results can provide more detailed information demonstrating infestations at various levels. The findings of this study can be applied to proximal sensing applications.

5. Conclusions

This research characterizes the hyperspectral response of coffee leaves affected by *Leucoptera coffeella* using a high-precision instrument in a case study conducted in Brazil. Our findings highlight the critical role of two wavelengths (700 nm and 630 nm) in distinguishing between symptomatic and healthy leaves. Furthermore, reflectance thresholds are established to classify leaf diseases and aim to lay the groundwork for an agronomic reference related to CLM. These results provide essential foundational knowledge and hold substantial implications for the scientific community, particularly in advancing more robust monitoring and detection systems. Moreover, these findings highlight the value of terrestrial hyperspectral data for comprehensive monitoring of CLM infestations, providing detailed and complementary information for more sustainable pest management in coffee.

References

1. FAO. *Crops and Climate Change Impact Briefs: Climate-Smart Agriculture for More Sustainable, Resilient, and Equitable Food Systems*; FAO: Roma, Italy, 2022. [CrossRef]

2.   Dantas, J.; Motta, I.; Vidal, L.; Bilio, J.; Pupe, J.M.; Veiga, A.; Santana, C.C.; Leite, D.H.; Matos, C.S.M. A Comprehensive Review of the Coffee Leaf Miner *Leucoptera coffeella* (Lepidoptera: Lyonetiidae), with Special Regard to Neotropical Impacts, Pest Management and Control. *Preprints* **2021**, *1*, 1–25. [CrossRef]
3.   Pantoja-Gomez, L.M.; Corrêa, A.S.; De Oliveira, L.O.; Guedes, R.N.C. Common Origin of Brazilian and Colombian Populations of the Neotropical Coffee Leaf Miner, *Leucoptera coffeella* (Lepidoptera: Lyonetiidae). *J. Econ. Entomol.* **2019**, *112*, 931–934. [CrossRef] [PubMed]
4.   Souza, J.C.; Reis, P.R.; Rigitano, R.L.O. *Bicho-Mineiro do Cafeeiro: Biologia, Danos e Manejo Integrado*, 2nd ed.; EPAMIG: Belo Horizonte, Brazil, 1998; Volume 54.
5.   Liu, W.H.; Dai, X.H.; Xu, J.S. Revisión de las Influencias de los Insectos Minadores de Hojas en sus Plantas Huésped. *Collect. Bot.* **2015**, *34*, 5. [CrossRef]
6.   Arteca, R.N. *Plant Growth Substances: Principles and Applications*; Springer: New York, NY, USA, 1996. [CrossRef]
7.   Zampiroli, R.; Alvarenga, C.B.; Andaló, V.; Rinaldi, P.C.; Assis, G.A. Application Technology for Chemically Controlling Coffee Leaf Miner in the Cerrado of Minas Gerais State. *Rev. Cienc. Agrar.* **2017**, *60*, 256–262. [CrossRef]
8.   Silva, B.K.R.; Malaquias, M.F.; Faria Filho, R.F.; Santos, A.V.F.; Fernandes, F.L. Spatial and Dynamic Distribution of Chrysoperla spp. and *Leucoptera coffeella* Populations in Coffee *Coffea arabica* L. *Precis. Agric.* **2023**, *25*, 327–346. [CrossRef]
9.   Ali, M.M.; Bachik, N.A.; Muhadi, N.A.; Norizan, T.; Yusof, T. Non-Destructive Techniques of Detecting Plant Diseases: A Review. *Physiol. Mol. Plant Pathol.* **2019**, *108*, 101426. [CrossRef]
10.   Sishodia, R.P.; Ray, R.L.; Singh, S.K. Applications of Remote Sensing in Precision Agriculture: A Review. *Remote Sens.* **2020**, *12*, 3136. [CrossRef]
11.   Weiss, M.; Jacob, F.; Duveiller, G. Remote Sensing for Agricultural Applications: A Meta-Review. *Remote Sens. Environ.* **2020**, *236*, 111402. [CrossRef]
12.   Hunt, D.A.; Tabor, K.; Hewson, J.H.; Wood, M.A.; Reymondin, L.; Koenig, K. Review of Remote Sensing Methods to Map Coffee Production Systems. *Remote Sens.* **2020**, *12*, 2041. [CrossRef]
13.   Martins, G.D.; Galo, M.L.B.T.; Vieira, B.S. Detecting and Mapping Root-Knot Nematode Infection in Coffee Crop Using Remote Sensing Measurements. *IEEE J. Sel. Top. Appl. Earth Obs. Remote Sens.* **2017**, *10*, 5395–5403. [CrossRef]
14.   Pereira, F.V.; Martins, G.D.; Vieira, B.S.; Assis, G.A.; Orlando, V.S.W. Multispectral Images for Monitoring the Physiological Parameters of Coffee Plants Under Different Treatments Against Nematodes. *Precis. Agric.* **2022**, *23*, 2312–2344. [CrossRef]
15.   Vilela, E.F.; Ferreira, W.P.M.; Castro, G.D.M.; Faria, A.L.R.; Leite, D.H.; Lima, I.A.; Santana, C.C.; Matos, C.S.M. New Spectral Index and Machine Learning Models for Detecting Coffee Leaf Miner Infestation Using Sentinel-2 Multispectral Imagery. *Agriculture* **2023**, *13*, 388. [CrossRef]
16.   Orlando, V.S.W.; Vieira, B.S.; Martins, G.D.; Lopes, E.A.; Assis, G.A.; Pereira, F.V.; Galo, M.L.B.T.; Rodrigues, L.S. Orbital Multispectral Imaging: A Tool for Discriminating Management Strategies for Nematodes in Coffee. *Precis. Agric.* **2024**, *25*, 2573–2588. [CrossRef]
17.   Vilela, E.F.; Castro, G.D.M.; Marin, D.B.; Santana, C.C.; Leite, D.H.; Matos, C.S.M.; Lima, I.A.; Faria, A.L.R.; Ferreira, W.P.M. Remote Monitoring of Coffee Leaf Miner Infestation Using Machine Learning. *AgriEngineering* **2024**, *6*, 1697–1711. [CrossRef]
18.   Sismet Cooxupé. Data Weather Stations. Available online: https://sismet.cooxupe.com.br:9000/dados/estacao/ (accessed on 28 November 2023).
19.   Jackson, R.D.; Clarke, T.R.; Moran, M.S. Bidirectional Calibration Results for 11 Spectralon and 16 BaSO4 Reference Reflectance Panels. *Remote Sens. Environ.* **1992**, *40*, 231–239. [CrossRef]
20.   Jorge, L.A.C.; Silva, D.J.C.B. AFSoft—Software para Análise Foliar. In Proceedings of the Congresso Brasileiro de Agricultura de Precisão—ConBAP, Ribeirão Preto, Brazil, 27–29 September 2010.
21.   Rousseeuw, P.J. Silhouettes: A Graphical Aid to the Interpretation and Validation of Cluster Analysis. *J. Comput. Appl. Math.* **1987**, *20*, 53–65. [CrossRef]
22.   Tsai, F.; Philpot, W. Derivative Analysis of Hyperspectral Data. *Remote Sens. Environ.* **1998**, *66*, 41–51. [CrossRef]
23.   Orlando, V.S.W.; Galo, M.D.L.B.T.; Martins, G.D.; Lingua, A.M.; Andaló, V. UAV Imaging for Spectral Characterization of Coffee Leaf Miner (Leucoptera coffeella) Infestation in the Cerrado Mineiro Region. *ISPRS Ann. Photogramm. Remote Sens. Spatial Inf. Sci.* **2024**, *X-3-2024*, 285–291. [CrossRef]
24.   Curran, P.J.; Dungan, J.L.; Macler, B.A.; Plummer, S.E. The Effect of a Red Leaf Pigment on the Relationship Between Red Edge and Chlorophyll Concentration. *Remote Sens. Environ.* **1991**, *35*, 69–76. [CrossRef]
25.   Martins, G.D. Inferência dos Níveis de Infecção por Nematoides na Cultura Cafeeira a Partir de Dados de Sensoriamento Remoto Adquiridos em Multiescala. Ph.D. Thesis, Universidade Estadual Paulista, Presidente Prudente, Brazil, 2016.
26.   Mahlein, A.-K.; Steiner, U.; Dehne, H.-W.; Oerke, E.-C. Spectral Signatures of Sugar Beet Leaves for the Detection and Differentiation of Diseases. *Precis. Agric.* **2010**, *11*, 413–431. [CrossRef]